

AD-764 489

A COLOR SCHLIEREN STUDY OF AMMONIUM  
PERCHLORATE AND AMMONIUM PERCHLORATE-  
BINDER SANDWICH COMBUSTION

James LeRoy Murphy, III

Naval Postgraduate School  
Monterey, California

March 1973

DISTRIBUTED BY:

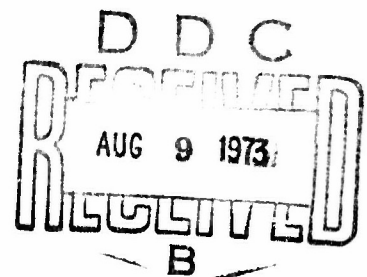
**NTIS**

National Technical Information Service  
U. S. DEPARTMENT OF COMMERCE  
5285 Port Royal Road, Springfield Va. 22151

AD 764489

# NAVAL POSTGRADUATE SCHOOL

Monterey, California



## THESIS

A COLOR SCHLIEREN STUDY OF  
AMMONIUM PERCHLORATE AND  
AMMONIUM PERCHLORATE-BINDER  
SANDWICH COMBUSTION

by

James LeRoy Murphy III

Thesis Advisor:

David W. Netzer

March 1973

Reproduced by  
NATIONAL TECHNICAL  
INFORMATION SERVICE  
U S Department of Commerce  
Springfield VA 22151

Approved for public release; distribution unlimited.

A Color Schlieren Study of  
Ammonium Perchlorate and  
Ammonium Perchlorate-Binder  
Sandwich Combustion

by

James LeRoy Murphy III  
Lieutenant, United States Navy  
B.S., United States Naval Academy, 1967

Submitted in partial fulfillment of the  
requirements for the degree of

MASTER OF SCIENCE IN AERONAUTICAL ENGINEERING

from the

NAVAL POSTGRADUATE SCHOOL  
March 1973

Author

*James L. Murphy III*

Approved by:

*David W. Nitzen*

Thesis Advisor

*Richard*

Chairman, Department of Aeronautics

*Milton H. Clauser*

Academic Dean

UNCLASSIFIED

Security Classification

## DOCUMENT CONTROL DATA - R &amp; D

(Security classification of title, body of abstract and indexing annotation must be entered when the overall report is classified)

1. ORIGINATING ACTIVITY (Corporate author) Naval Postgraduate School Monterey, California 93940		2a. REPORT SECURITY CLASSIFICATION Unclassified	
		2b. GROUP	
3. REPORT TITLE A Color Schlieren Study of Ammonium Perchlorate and Ammonium Perchlorate-Binder Sandwich Combustion			
4. DESCRIPTIVE NOTES (Type of report and, inclusive dates) Master's Thesis; March 1973			
5. AUTHOR(S) (First name, middle initial, last name) James LeRoy Murphy III			
6. REPORT DATE March 1973		7a. TOTAL NO. OF PAGES 67	7b. NO. OF REFS 7
8a. CONTRACT OR GRANT NO.		8a. ORIGINATOR'S REPORT NUMBER(S)	
b. PROJECT NO.			
c.		8b. OTHER REPORT NO(S) (Any other numbers that may be assigned this report)	
d.			
10. DISTRIBUTION STATEMENT Approved for public release; distribution unlimited			
11. SUPPLEMENTARY NOTES		12. SPONSORING MILITARY ACTIVITY Naval Postgraduate School Monterey, California 93940	
13. ABSTRACT Single crystal and pressed polycrystalline ammonium perchlorate and ammonium perchlorate-binder (polybutadiene acrylic acid, hydroxyl terminated polybutadiene, polyurethane, and carboxyl terminated polybutadiene) sandwiches were burned in a nitrogen-purged combustion bomb at pressures above and below the lower pressure deflagration limit of ammonium perchlorate. High-speed color schlieren and regular motion pictures were taken of the combustion process in order to determine the effects of pressure, binder type, binder thickness, and purity of ammonium perchlorate on the deflagration.			

UNCLASSIFIED

Security Classification

A-81408





## ABSTRACT

Single crystal and pressed polycrystalline ammonium perchlorate and ammonium perchlorate-binder (polybutadiene acrylic acid, hydroxyl terminated polybutadiene, polyurethane, and carboxyl terminated polybutadiene) sandwiches were burned in a nitrogen-purged combustion bomb at pressures above and below the lower pressure deflagration limit of ammonium perchlorate. High-speed color schlieren and regular motion pictures were taken of the combustion process in order to determine the effects of pressure, binder type, binder thickness, and purity of ammonium perchlorate on the deflagration.

## TABLE OF CONTENTS

I.	INTRODUCTION -----	9
II.	METHOD OF INVESTIGATION -----	11
III.	DESCRIPTION OF APPARATUS -----	12
IV.	EXPERIMENTAL PROCEDURE -----	15
V.	RESULTS AND DISCUSSION -----	16
	A. PREVIOUS RESULTS -----	16
	1. PBAA -----	16
	2. HTPB -----	16
	3. PU -----	17
	4. CTPB -----	17
	B. DATA SUMMARY -----	17
	C. AMMONIUM PERCHLORATE DEFLAGRATION -----	18
	D. AMMONIUM PERCHLORATE - BINDER SANDWICH COMBUSTION -----	23
	1. Effect of Binder Composition -----	23
	2. Effect of Binder Thickness -----	25
	3. Effect of Pressure -----	27
	4. Effect of AP Purity -----	30
VI.	CONCLUSIONS -----	32
	A. EFFECT OF PRESSURE -----	32
	B. EFFECT OF BINDER COMPOSITION -----	33
	C. EFFECT OF BINDER THICKNESS -----	33
	D. EFFECT OF AMMONIUM PERCHLORATE PURITY -----	33

E. EFFECT ON MODELING -----	33
LIST OF REFERENCES -----	63
BIBLIOGRAPHY -----	64
INITIAL DISTRIBUTION LIST -----	65
FORM DD 1473 -----	66

## LIST OF TABLES

Table	Page
I. Binder Data -----	35
II. Tests Conducted -----	36
III. Conditions for Experimental Runs -----	37
IV. Experimental Run Data -----	38-39
V. Summary of Data from Films -----	40-43

## LIST OF FIGURES

Figure	Page
1. Schematic of Equipment Arrangement -----	44
2. View of Equipment Arrangement -----	45
3. Sandwich Burner Dimensions -----	46
4. PP-UHP AP Burned at 400 psig -----	47
5. SC-UHP AP Burned at 400 psig -----	47
6. PP-COMM AP Burned at 400 psig -----	48
7. PF-UHP AP Burned at 500 psig -----	48
8. SC-UHP AP Burned at 500 psig -----	49
9. PP-COMM AP Burned at 500 psig -----	49
10. PP-UHP AP Burned at 800 psig -----	50
11. SC-UHP AP Burned at 800 psig -----	50
12. PP-UHP AP/PBAA, 94 micron binder, 100 psig -----	51
13. PP-UHP AP/PBAA, 50 micron binder, 300 psig -----	51
14. PP-UHP AP/PBAA, 80 micron binder, 300 psig -----	52
15. PP-UHP AP/PBAA, 94 micron binder, No Side Lighting, 300 psig -----	52
16. PP-UHP AP/PBAA, 432 micron binder, 300 psig -----	53
17. PP-UHP AP/PBAA, 86 micron binder, 400 psig -----	53
18. PP-UHP AP/PBAA, 47 micron binder, 500 psig -----	54
19. PP-UHP AP/PBAA, 94 micron binder, 500 psig -----	54
20. PP-UHP AP/PBAA, 439 micron binder, 500 psig -----	55
21. PP-UHP AP/PBAA, 76 micron binder, 600 psig -----	55

Figure	Page
22. PP-UHP AP/HTPB, 64 micron binder, 300 psig -----	56
23. PP-UHP AP/HTPB, 93 micron binder, 300 psig -----	56
24. PP-COMM AP/HTPB, 100 micron binder, 300 psig -----	57
25. PP-UHP AP/HTPB, 37 micron binder, 500 psig -----	57
26. PP-UHP AP/HTPB, 94 micron binder, 500 psig -----	58
27. PP-COMM AP/HTPB, 99 micron binder, 500 psig -----	58
28. PP-UHP AP/PU, 114 micron binder, 300 psig -----	59
29. PP-UHP AP/PU, 116 micron binder, 500 psig -----	59
30. SC-UHP AP/CTPB, 192 micron binder, 300 psig -----	60
31. SC-UHP AP/CTPB, 55 micron binder, 500 psig -----	60
32. SC-UHP AP Burned at 1000 psig -----	61
33. SC-UHP AP Burned at 500 psig with a Horizontal Color Matrix	61
34. SC-UHP AP, 200 psig, Wire-wrapped Crystal -----	62
35. PP-UHP AP/HTPB, 61 micron binder, 500 psig, Color Matrix Removed -----	62

### ACKNOWLEDGEMENT

This work was sponsored by Naval Ordnance Systems Command, ORD  
TASK 331-007/551-1-332.

I would like to acknowledge the help of Professor D. W. Netzer and Mr. Edward Michelson for their assistance and advice throughout the course of this project. Appreciation is also due Mr. Thomas L. Boggs of the Naval Weapons Center, China Lake, for supplying the needed propellant ingredients and grown crystals. Finally, but not least in importance, much appreciation is expressed for the support, help, and patience shown by my wife.



## I. INTRODUCTION

Many analytical and experimental studies have been made of composite solid propellants which use ammonium perchlorate (AP) as the oxidizer. These have been reviewed by numerous investigators, e.g., Varney [Ref. 1]. In addition, considerable effort has been made to understand AP deflagration and AP-binder sandwich combustion. Two dimensional propellant sandwiches have been used in order to provide a convenient means of studying a variety of propellant types under a wide range of test conditions, and they allow AP-binder interactions to be conveniently studied by visual methods.

While much has been learned about AP and AP-binder sandwich decomposition and deflagration, many questions remain unanswered. Two such questions are concerned with the effects of pressure and binder composition on flame type (premixed or diffusion), and flame characteristics (laminar, turbulent, steady, or nonsteady). If adequate modeling of propellant combustion is to be obtained, the answers to these questions are required.

In the past, most studies of AP-binder sandwich combustion have been conducted by using high-speed motion picture photography of deflagrating propellant samples, and post-fire examination of quenched samples [Ref. 1, 2, 3, 4, 5]. In order to gain further needed knowledge of the behavior (surface configuration, etc.) of AP during deflagration,

Kennedy [Ref. 6] conducted a schlieren investigation of AP-binder sandwich combustion. He found (1) a complex interaction occurs between the primary flame, AP deflagration, and binder pyrolysis products, (2) the sandwich burner flames are laminar below the lower pressure deflagration limit (PDL) of AP and appeared to be unsteady or "turbulent" above the PDL of AP, and (3) two distinct multiple flame regions exist, one above the binder and one near the binder-AP interface. Limitations of his study were (1) the use of a schlieren optical depth that allowed much flame averaging to occur, (2) an object-to-image magnification ratio of 3:1, which did not allow sufficient resolution of the burning process, (3) separate schlieren and real-light films of different propellant burners, burning under similar conditions, and (4) the use of only one grade of AP and of only one type of binder and binder thickness.

In this investigation, some of the refinements made to the apparatus and the techniques used by Kennedy were (1) a higher object-to-image magnification ratio on the film, (2) color schlieren and real-light photography of a single sandwich burner on the same film, and (3) a smaller sandwich burner to reduce the schlieren optical path length through the flame, thereby reducing the averaging effect on the schlieren photography.

The purposes of this investigation were (1) to refine the experimental apparatus and the techniques used by Kennedy in order to improve the quality of the experimental data and (2) to use the improved methods to study AP deflagration and AP-binder sandwich combustion for various purities of AP and types and thicknesses of binder.

## II. METHOD OF INVESTIGATION

Propellant sandwiches were made from three grades of pressed polycrystalline AP and three different types of binder. The grades of AP were ultra-high purity (UHP), commercial grade, and commercial grade with tricalcium phosphate (TCP) added as an anti-caking agent. The three binders used were polybutadiene acrylic acid (PBAA), polyurethane (PU), and hydroxyl terminated polybutadiene (HTPB). The binder thicknesses were varied from 25 microns to 508 microns for sandwiches of PBAA. For sandwiches of PU a binder thickness of 51 microns was used. For sandwiches of HTPB the binder thicknesses were varied from 25 microns to 51 microns. Sandwiches made from single crystals of AP and carboxyl terminated polybutadiene (CTPB) were also studied.

In addition to the sandwich studies, single crystal AP and pressed polycrystalline AP were also studied.

Tests were conducted in a nitrogen purged combustion bomb at pressures from 100 to 1000 psig.

A high-speed (7500 PPS) color motion picture was taken for each test condition. Each film contained alternating frames of color schlieren and standard real-light color pictures. The films were analyzed to determine the effects of binder type, binder thicknesses, AP type and purity, and combustion pressure on the flame and burning surface characteristics.

### III. DESCRIPTION OF APPARATUS

The combustion bomb used in this study was fabricated of stainless steel and was hydrostatically tested to 1500 psi. The bomb had integral provisions for mounting and igniting the sandwich burners and for purging the bomb during combustion with a flow of nitrogen gas. Reference 6 contains diagrams, photographs, and schematics of the combustion bomb and its associated apparatus.

Previous work done at the Naval Postgraduate School [Ref. 6] with the combustion bomb described above used a 203-millimeter lens to focus the image of the deflagrating sandwich burner onto the film plane of the high-speed motion picture camera. This lens was found to be inadequate for the detailed picture of the flame needed in this study. Consequently, a 610-millimeter lens was substituted and a magnification of 0.8 was achieved on the film plane.

The alignment of the schlieren light source, the various lenses, the combustion bomb, and the camera was critical. To facilitate the alignment procedure, an Optics-Technology He-Ne laser was used to ensure that the lenses, bomb, and light source were in as straight a line as possible. Once aligned, the optical bench holding the lenses was bolted down and the light source and lenses were not moved for the remainder of the study. The camera was substituted for the laser and was placed at the focal length of the focusing lens. Figure 1 is a schematic of the arrangement of the various components.

In earlier studies a color matrix constructed by placing a red and a blue gelatin filter between two plates of glass was used to produce the color schlieren. However, it was felt that this technique could be distorting the color schlieren and that the gelatin filters had a tendency to mold. To reduce these problems to a minimum, a color slide photograph of the red and blue gelatin filters between two plates of glass was used to produce the color schlieren.

In order to make high-speed motion pictures in which both schlieren and real-light photography of a single burner could be made, a light-source chopper was designed and constructed. It was turned by a small electric motor and, at full camera speed, allowed approximately four frames of real-light photography alternated with four frames of schlieren photography.

A model K2004E-115 Hycam camera with variable framing rates from 1000 to 10,000 pictures per second and a pulse timer were used to take the schlieren and real-light photography. Kodak Ektachrome 7241, ASA 40, high speed color film was used for all photography.

The light source for the real-light photography was a modified Spindler and Sauppe Inc., Selectroslide, model SLM-1200 (1200 watt) slide projector aimed through the  $45^{\circ}$  window of the combustion bomb. The light source for the schlieren photography was a 1000-watt mercury arc lamp.

A 610-millimeter lens was used to focus the sandwich image directly onto the film plane of the camera.

Combustion bomb pressurization, burner ignition, and camera activation were controlled from behind a safety shield [See Fig. 2].

The polycrystalline AP and the ingredients for the various binders were weighed (separately) in a Mettlers, type H-15, 160 gram capacity balance. The polycrystalline AP was then placed in a compaction mold [Ref. 6] for pressing in a 24,000 pound capacity hydraulic press.

Prepared sandwich burners were measured for height, width, binder thickness, and optical depth [See Fig. 3] with a Gaertner Scientific Corporation microscope. Binder thickness determination in earlier work done at the Naval Postgraduate School was accomplished by direct measurement from the projected image of the burning sandwich.

#### IV. EXPERIMENTAL PROCEDURE

Burner fabrication required considerable time. The AP was weighed, placed in the compaction mold, and subjected to 30,500 psi for 20 minutes. This resulted in a polycrystalline wafer of AP approximately 1.27 millimeters thick with a diameter of 25.4 millimeters, and a density of better than 97% of the pure crystal density. Two wafers of AP were then coated on one side with binder, placed together to form a sandwich, and then placed in an oven and cured as indicated in Table I. The first three hours of cure were done in a vacuum of better than 28 inches of mercury in all cases. After cure, the sandwich was scribed and then cleaved into six burners. Each burner then had to be scraped with a sharp blade until an optical depth of from 1.18 millimeters to 1.44 millimeters was attained. Finally, the burner was mounted on a pedestal with glue.

Ignition of the burners was accomplished by means of a nichrome resistance wire laid across the top of the burner and then heated by passing current from a 12-volt battery through the wire.

The image of the sandwich burner was then focused onto the film plane of the camera by moving the 610-millimeter focusing lens [See Fig. 1]. The focus was critical since the depth of field of the 610-millimeter lens was of the same order as the optical depth of the sandwich burners.

Table II presents a summary of the tests conducted in this investigation. Table III presents a summary of the conditions under which the tests were conducted.

## V. RESULTS AND DISCUSSION

### A. PREVIOUS RESULTS

Before proceeding with the results of this investigation, a brief summary of some results of other investigations for AP sandwich burners with PBAA, HTPB, PU, and CTPB are presented [Ref. 1, 2, 6, and 7].

#### 1. PBAA

a. Melted PBAA flows over some of the AP, the amount of AP covered being dependent on pressure.

b. The binder-oxidizer interface is smooth, i e., there are no significant interfacial reactions.

c. The maximum surface regression occurs in the AP in the pressure range from the PDL of AP (approximately 300 psi) to 1000 psi.

d. At a binder thickness somewhere below 50 microns, a "hump of AP" (covered with molten binder) can occur and gives asymmetrical burning. This effect was not so predominant in Varney's work [Ref. 1].

e. A liquid layer is present on the AP during combustion at pressures above the PDL of AP.

#### 2. HTPB

a. The melted binder is quite viscous and flow is limited to the proximity of the original binder interface.

b. The melted binder and the liquid due to AP deflagration do not mix appreciably.



c. Below the PDL of AP, the sandwiches regress with a notched surface appearance and a laminar diffusion flame.

d. As pressure is increased, the AP regresses more rapidly than does the binder, leaving the binder protruded above the surface.

### 3. PU

a. Melted PU flows over the AP adjacent to the binder. This PU melt inhibits the sandwich regression.

b. Sandwich regression is not markedly dependent upon binder thickness.

c. The binder pyrolysis products are relatively non-reactive.

d. There is no evidence of binder-oxidizer interfacial reactions.

### 4. CTPB

a. Melted CTPB flows over the AP adjacent to the binder. This CTPB melt inhibits the sandwich regression.

b. The amount of melt is dependent on the pressure and binder thickness.

c. One side of the sandwich typically lags behind the other during deflagration.

d. There are no significant interfacial reactions between binder and oxidizer.

## B. DATA SUMMARY

Table IV shows the runs made in compiling the data for this study. Table V summarizes the experimental findings which are discussed below.

Films 27 through 64 provided the necessary data for determination of the effects of pressure, binder type, binder thickness, and AP purity on combustion characteristics. Film 51, omitted from Table III, was of a very wide wafer of pressed polycrystalline AP. It was burned in order to determine if the flow of nitrogen in the combustion bomb had any effect on the temperature profile as shown by the schlieren photography. There was no noticeable effect.

Two runs with sandwiches made from HTPB and pressed polycrystalline AP with TCP added were attempted at pressures of 300 psig and 500 psig. Neither achieved successful ignition at these pressures, and, therefore, were not included in the tabulated data.

#### C. AMMONIUM PERCHLORATE DEFLAGRATION

The PDL for the various grades of AP burning as a monopropellant was determined prior to any data points being run. UHP and commercial grade AP had the same PDL, approximately 355 psig. All attempts to ignite AP with TCP in the pressure range from 100 psig to 1000 psig were unsuccessful.

Single crystal and pressed polycrystalline wafers of AP were burned without binder in order to gain some insight into the deflagration of AP as a monopropellant before trying to interpret AP sandwich data.

Figures 4, 5, and 6 are color schlieren photographs taken at 400 psig of pressed polycrystalline ultra-high purity (PP-UHP) AP, single crystal ultra-high purity (SC-UHP) AP, and pressed polycrystalline

commercial grade (PP-COMM) AP respectively. The blue to red color shifts just above the burner surface for all types of AP should be noted. These sites are on the order of 300 microns in width. The deflagration of all three burners appears laminar, with a definite temperature peak above the center of the burner. The scalloped surface of the PP-COMM AP is thought to account for the more unsteady appearance of the gas flow above the deflagrating AP in Fig. 6. In Fig. 5 a yellow-green zone is visible in the crystal, extending from the burner surface to a depth of approximately 200 microns. This zone is thought to be related to the phase change from an orthorhombic crystalline structure to a cubic structure (the  $243^{\circ}\text{C}$  isotherm) as reported by Boggs and Kraeutle [Ref. 4], Hightower and Price [Ref. 2], and Beckstead and Hightower [Ref. 8]. Beckstead and Hightower found this phase change zone to be approximately 22 microns deep in single crystals of AP burned at pressures of 400 psi. The three studies mentioned above investigated quenched samples to determine the phase change zone thickness. The difference between their results and the results of this study may be due to removal of surface material during quench and/or to an inaccurate measurement of the penetration depth of the cubic structure obtained from the recrystallized quenched samples. More likely, however, is the possibility of light scattering (due to small cracks, etc.) and/or other than phase change phenomena causing the larger thickness found in this investigation.

Figures 7 through 9 are color schlieren photographs taken at 500 psig of PP-UHP AP, SC-UHP AP, and PP-COMM AP respectively. The gases

above the deflagrating AP are more turbulent in appearance than at 400 psig. There is much more large scale mixing closer to the burner surface than at 400 psig. The characteristic alternating red and blue zones are again visible and are on the order of 300 to 400 microns in width. The subsurface zone in Fig. 8 appeared to be thinner than the zone in Fig. 5, but was not well enough defined for accurate measurement.

Figures 10 and 11 are color schlieren photographs taken at 800 psig of PP-UHP AP, and SC-UHP AP respectively. Deflagration is now clearly turbulent, with a more uniform temperature in the gases above the burner, as evidenced by the lack of a definite temperature peak and by the alternating red and blue tongues of color rising from the burner surfaces and extending upwards for some distance above the burner surfaces. The subsurface zone was very thin at 800 psig.

Figure 32 is a color schlieren photograph taken at 1000 psig of a SC-UHP AP burner. Deflagration is extremely turbulent as is evidenced by an almost uniform color in the gases just above the burner surface. The subsurface zone was not visible at this pressure. Careful examination of the film revealed the presence of alternating red and blue color shifts very close to the surface. These color shifts were estimated to be on the order of 150 microns in width but were very difficult to measure because of their small size.

Comparison of Figures 5, 8, 11, and 32 indicated that the thickness of the subsurface zone associated with the phase change (and/or other

phenomena) decreased as pressure was increased in agreement with the results reported by Beckstead and Hightower [Ref. 8].

Two additional tests were made in order to further study the subsurface zone. Figure 33 shows a color schlieren photograph taken at 500 psig of SC-UHP AP in which the color matrix was horizontally positioned. The schlieren thus indicates density (temperature) gradients only in the direction normal to the burning surface. The same subsurface yellow-green colored zone is evident, indicating that the green color results from the back lighting through the altered crystal structure (the mercury light source has several strong lines in the yellow-green frequency range) and is not due to schlieren effects. The red color above the surface indicates the increasing temperature.

Another interesting observation was made from the film from which Fig. 33 was taken. The AP appeared to be burning in a pulsating, thermal layer manner. The red color above the crystal evolved like puffs of smoke from the entire surface.

One additional test was made to investigate the subsurface zone. A single pure crystal of AP was wrapped with a resistance wire and the wire heated to approximately  $250^{\circ}\text{C}$  with a bomb pressure of 200 psig (below the PDL of AP). Figure 34 shows that where the wire touched the crystal (left side) the yellow-green color is evident.

These results indicate that the yellow-green subsurface region is definitely associated with the orthorhombic to cubic phase change.

The blue to red alternating color shifts across the burner surface mentioned above are thought to result from local zones of rapid density (or temperature) change, i.e., local reaction sites on the surface of the AP. Such local reaction sites have been reported by Boggs and Kraeutle [Ref. 4], and Hightower and Price [Ref. 2]. Hightower and Price report surface depressions on the order of 150 microns in width on the burner surface of quenched samples burned in the range of 300 to 700 psi. The width of the blue to red color shifts measured from schlieren photographs taken in this study were about 300 microns in width. These blue to red color shifts may either be local reaction sites that merge together or may be indicating the distance between sites. The dimensions of the spaces between reaction sites were observed to be relatively independent of pressure in the range from 400 to 800 psig. However, there was a marked change in the appearance of the gases above the deflagrating surface when the pressure was raised from 800 psig to 1000 psig. The distinct sites which existed at 800 psig became quite small or nonexistent at 1000 psig. Boggs and Kraeutle [Ref. 4] found from quenched AP that the surface structure changed between 800 and 1000 psi. Below 800 psi a continuous bubbling froth existed on the surface. At 1000 psi the froth was found only in the valleys of a closely spaced (approximately 75 microns) ridge-valley surface structure. Thus, the schlieren observations of the gas phase during combustion appear to agree with the results obtained from quenched samples.

The purity of the AP and whether a single crystal or polycrystalline wafer was used appeared to have no effect on the width of the spaces between the sites.

#### D. AP-BINDER SANDWICH COMBUSTION

Figures 12 through 31 present color schlieren photographs taken of the various AP-binder sandwich tests which are summarized in Table V.

In the paragraphs that follow, the effects of binder type, binder thickness, AP purity, and pressure on the characteristics of the sandwich deflagration will be discussed. When referring to binder thicknesses, "thin" will be used to describe a thickness of less than 64 microns, "medium" will be used to describe binder thicknesses of about 100 to 200 microns, and "thick" will be used for binder thicknesses of approximately 400 microns.

The data obtained from the burning of the SC-UHP AP with CTPB were not used in the analysis since the optical depth of the sandwich burners used was much larger than the optical depth of the pressed polycrystalline sandwich burners, allowing much averaging through the flame to occur.

##### 1. Effect of Binder Composition

Figures 13 and 22 are color schlieren photographs of PP-UHP AP with PBAA and HTPB binders respectively. The binder thicknesses are thin and the pressure is 300 psig. This pressure is below the PDL of AP. Comparison of the two shows that both are burning with a small laminar



flame. A peak temperature exists in the gases above the visible flame located above the binder. The peak temperature above the binder is the result of the cool nitrogen atmosphere within the combustion bomb and a single closed (visible) flame above the binder.

Comparison of Fig. 14 (PP-UHP AP with PBAA), Fig. 23 (PP-UHP AP with HTPB), and Fig. 28 (PP-UHP AP with PU), all with medium binder thickness, and taken at a pressure of 300 psig, shows that all are burning with a closed flame with a well-defined peak temperature at the center above the binder. The combustion of the PBAA sandwich (Fig. 14) and the HTPB sandwich (Fig. 23) appeared to be very similar. Both exhibited a relatively large single visible flame. The AP deflagration from the burner surfaces was laminar. The PU sandwich (Fig. 28) burned with a very small flame and the AP deflagration appeared more turbulent than for either the PBAA or HTPB sandwiches. This was felt to be due to the binder melt flowing over the AP surface as noted by Boggs and Zurn (Ref. 7).

Comparison of the schlieren photographs of sandwiches of PBAA and HTPB with a thin binder thickness, taken at 500 psig (Fig. 18 and 25) show that the gases above the sandwich are very close to being turbulent in both cases. No significant difference was evident for the two binders. In both cases the visible flame was actually two flames, one on each side of the binder protruding above the burner surfaces. This causes the double blue-to-red shift seen in these photographs with a temperature minimum above the protruding binder. The visible flames for the PBAA and the HTPB binders are both approximately the same size.



Comparison of PBAA, HTPB, and PU sandwiches taken at 500 psig with a medium binder thickness (Fig. 19, 26, and 29) shows all have approximately the same degree of visible flame "turbulence" and size, with perhaps the PBAA visible flame being slightly taller than the other two. All three exhibited the two flame structure mentioned above for the thin binder case. The PU sandwich surface was almost flat as compared to the slight concave surfaces of the PBAA and HTPB sandwiches. This was once again attributed to the flow of PU binder melt over the AP surface. The visible flame of the PU sandwich appeared more laminar than either the PBAA or HTPB sandwiches, but the gases above the AP appeared slightly turbulent for all three burners.

In summary, sandwiches made with PBAA and HTPB behave in a very similar fashion with small amounts of binder flow. However, PU appears to flow readily over the adjacent AP surface, causing the gases evolving from the surface to be more turbulent and the surface regression to be more planar.

## 2. Effect of Binder Thickness

Variation of the binder thickness for sandwiches of PU were not studied.

Comparison of PBAA sandwiches taken at 300 psig for thin, medium, and thick binder thicknesses (Fig. 13, 14, and 16) indicates that increasing the binder thicknesses at this pressure tends to force the deflagration to have a more laminar appearance. Also the visible flame height and width increased as the binder thickness was increased. The

more laminar appearance and the larger flames associated with the larger binder thicknesses appear to result from an increased binder protrusion height with thicker binders. Figures 18 through 20 are photographs of PBAA sandwiches taken at 500 psig for binder thicknesses ranging from thin to thick. The trend is seen to be the same as that discussed above for 300 psig, with the exception that the larger binder thickness does not seem to force the deflagration toward a laminar appearance. The visible flame for all binder thicknesses at 500 psig exhibited the two flame structure. The gases above the AP appeared to be somewhat turbulent for the 500 psig cases.

Figures 22 and 23 are color schlieren photographs of HTPB sandwiches taken at 300 psig with thin and medium binder thicknesses respectively. Once again, the trend was the same as for the PBAA sandwiches discussed above. The data collected at 500 psig for HTPB sandwiches with thin and medium binder thicknesses (Fig. 25 and 26) provided further verification of the trends mentioned above. Once again, the two flame structure for the visible flame was observed for both binder thicknesses.

In summary, increasing binder thickness appears to increase the binder protrusion height above the AP surface. The increased binder height causes larger visible flames and at pressures below the PDL of AP has a quiescent effect on the gases evolving from the surface.

### 3. Effect of Pressure

Comparison of Fig. 12, 14, 17, 19, and 21 for a medium binder thickness of PBAA, with pressures ranging from 100 psig to 600 psig shows a marked change in the steadiness of the gases evolving from the burner surfaces. To approximately 500 psig (Fig. 19) there is a discernible single temperature peak in the combustion gases which is located above the binder. Large scale mixing becomes more and more pronounced as the pressure is increased. The regression rate of the AP increased as pressure was increased as was evidenced by the flattening of the burner surface as pressure was increased above the PDL of AP. As pressure was increased from 100 to 400 psig, the flame height increased. From 400 to 500 psig, the flame height dropped and the visible flame transitioned from the single closed structure to the two flame structure. This resulted from the increased protrusion of the binder above the burner surface. At approximately 500 psig the gases above the AP became turbulent.

For the thin binder thickness (Fig. 13 and 18), the deflagration appears more turbulent at 300 psig than at 500 psig. This apparent anomaly is explained by the deep, rounded notch burned into the surface of the burner at 300 psig, which causes much large scale mixing of the AP decomposition products. Close investigation showed a large amount of mixing close to the burner surface at 500 psig, which is above the PDL of AP. Otherwise, the same trends as those discussed above for the medium binder thickness were observed.

Figures 16 and 20 are color schlieren photographs of PBAA sandwiches with a thick binder, taken at 300 and 500 psig respectively. The same trends as those discussed above for medium and thin binder thicknesses were observed, except that the large binder protrusion tended to stabilize the visible flame and the gases above the AP surface.

Figures 22 and 25 are color schlieren photographs of HTPB sandwiches with a thin binder, taken at 300 and 500 psig respectively. The same trends as for the PBAA sandwiches were observed. At 500 psig a very distinct two flame structure can be observed with a temperature minimum above the binder. Figures 23 and 26 show medium binder thickness HTPB sandwiches burned at 300 and 500 psig respectively. Once again the same trends as for the PBAA sandwiches were noted, with the exception that the flame height decreased as pressure was increased.

Figures 28 and 29 are color schlieren photographs of PU sandwiches of medium binder thickness taken at 300 and 500 psig respectively. The visible flame size can be seen to increase noticeably with pressure. The deflagration appears turbulent at 300 psig, possibly due to binder melt flowing over the AP. At 500 psig there is much large scale mixing and a much more turbulent appearance of the deflagration. The two flame structure is evidenced by the indication of a minimum temperature in the gases directly above the binder.

From the above results, it was concluded that the turbulence level in AP decomposition products increased as pressure was increased from below to above the PDL of AP. It was also concluded that, at

pressures below the PDL of AP, the visible flame has a single closed structure with one peak temperature in the center above the binder. As the pressure is increased above approximately 350 psig the AP begins to deflagrate. At a pressure somewhere between 400 and 500 psig (depending on binder type, etc.) the AP begins to deflagrate more rapidly than the AP-binder flame, leaving a protruding binder post. Once this occurs, the single closed flame is divided into the two flame structure, one on each side of the binder post. These flames do not rise vertically above the surface but, rather, are canted outward over the deflagrating AP as a result of the binder post. Thus, even without appreciable binder flow onto the AP, the visible flames become unsteady or "turbulent" as a result of the AP deflagration products interacting with the AP-binder diffusion flame. Binder flow onto the AP further aggravates the situation, causing more visible "turbulence."

One last item deserves mention in this section. In nearly all of the photographs shown in Fig. 4 through Fig. 33, a distinct yellow-green color is always present in the gas phase with some blue color adjacent to it. Also, it seems to form in abundance when any irregular portion of the sandwich protrudes well above the region of maximum surface regression. The yellow-green color was observed to occur with all AP crystals, including the single crystal burners. Fig. 35 is a photograph of a PP-UHP AP with HTPB sandwich burned at 500 psig with the schlieren color matrix removed. Therefore, it is a back lighted (with the mercury arc lamp) photograph. Light yellow streaks are present in the gas phase. This

yellow color with the blue schlieren color may be causing the yellow-green color in the gas phase. It is felt that this bright yellow-green color is linked to the phase change of AP from an orthorhombic structure to a cubic structure which occurs at approximately  $243^{\circ}\text{C}$ , although no proof of this conjecture can be offered except the observation of the same color in the single crystal AP just below the surface. Another possible explanation of the phenomenon is the emission or absorption of light by some product of the AP decomposition since the emission spectra of a mercury vapor arc lamp shows strong lines in the yellow-green region.

#### 4. Effect of AP Purity

Figures 23 and 24 are color schlieren photographs of PP-UHP AP with HTPB and PP-COMM AP with HTPB respectively. Both had a medium binder thickness and were burned at 300 psig. The PP-COMM burner surface exhibited the extreme notching characteristic of all burns made with commercial grade AP in this study. Evidently the AP deflagration rate for commercial grade AP is less than UHP AP even though the lower PDL for both are essentially the same. This notching leads to much surface generated turbulence for the commercial grade AP.

Figures 26 and 27 are color schlieren photographs of PP-UHP AP with HTPB and PP-COMM AP with HTPB respectively. Both had a medium binder thickness and were burned at 500 psig. The same tendencies that were observed for the 300 psig case were noted for this case.

It was concluded from the above that impurities in commercial grade AP (notably sulfated ash) inhibit deflagration rate and increase the

turbulence level of the combustion due mainly to the irregular surface configuration.

## VI. CONCLUSIONS

### A. EFFECT OF PRESSURE

In AP-binder sandwich deflagration, the turbulence level of gases evolving from the burner surface increases as pressure is increased from below to above the PDL of AP.

The subsurface crystal structure change zone decreases in thickness with increasing pressure and was not detectable at 1000 psig.

AP appears to burn in a pulsating, thermal layer manner.

Schlieren observations of deflagrating AP agree with the results obtained from quenched samples. The distinct change in the AP surface structure observed by Boggs and Kraeutle [Ref. 4] when increasing pressure from 800 to 1000 psi (from a continuous bubbling froth to a fine ridge-valley structure with froth in the valleys) was readily apparent in the gas phase with color schlieren photography. Below 800 psig, distinct reaction sites on the AP surface are approximately constant in size and are also readily apparent in the color schlieren photography.

At pressures below that which yields a planar sandwich regression, the visible flame is a closed laminar flame. As pressure is increased, a binder post protrudes above the regressing surface and splits the flame into two regions, one on each side of the binder post. These canted flames interact with the AP deflagration products causing a visibly "turbulent" flame. Binder flow onto the AP appears to augment the level of turbulence.



## B. EFFECT OF BINDER COMPOSITION

Sandwiches made with PBAA and HTPB behave in a very similar fashion with small amounts of binder flow. However, PU appears to flow readily over the adjacent AP surface, causing the gases evolving from the surface to be more turbulent and the surface regression to be more planar.

## C. EFFECT OF BINDER THICKNESS

Increasing binder thickness appears to increase the binder protrusion height above the AP surface. The increased binder height causes larger visible flames and at pressures below the PDL of AP has a quiescent effect on the gases evolving from the surface.

## D. EFFECT OF AMMONIUM PERCHLORATE PURITY

In all tests, the turbulence level was increased by decreasing the purity of the AP. This was observed to be the result of an increase in the irregularity of the burner surface as the purity of the AP was decreased. The contribution of an uneven burner surface to the turbulence level decreased as pressure was increased since the burner surface became more and more planar with increasing pressure, regardless of the purity of the AP.

## E. EFFECT ON MODELING

Because the turbulence level of sandwich combustion appeared to be a function of surface geometry as well as of pressure and the degree of binder flow onto the AP, effective modeling of solid fuel rocket propellants will be difficult.

In conclusion, high-speed color schlieren photography has been shown to be a valuable tool in the study of AP and AP-binder sandwich combustion. Behavior postulated from normal photography and quenched sample examination have been confirmed by examining the temperature profiles in the gas phase during actual combustion.

TABLE I

## BINDER DATA

## PBAA

Batch No.	PBAA (gm)	EPON 828 (gm)	Cure Time (hr)	Cure Temp (°C)
1	3.2041	0.6147	96.0	72
2	3.2041	0.6147	97.3	72
3	3.2041	0.6147	96.0	72
4	3.2041	0.6147	96.0	72
5	3.2041	0.6147	96.0	72
6	3.2041	0.6147	96.0	72
7	3.2041	0.6147	96.0	72

## HTPB

Batch No.	HTPB (gm)	IPDI (gm)	Cure Time (hr)	Cure Temp (°C)
1	3.0000	0.2000	96.0	60
2	3.0000	0.2000	96.0	60
3	3.0000	0.2000	168.0	60
4	3.0000	0.2000	168.0	60

## PU

Batch No.	Adiprene (gm)	Castor Oil (gm)	1,4 Butane Diol (gm)	Cure Time (hr)	Cure Temp (°C)
1	7.2000	2.7900	0.0100	120.0	48

TABLE II

## TESTS CONDUCTED

Propellant	Binder Type	Binder Thickness (microns)	Pressure (psig)
PP-UHP AP <sup>1</sup>	----	----	300, 320, 330 340, 345, 348 350, 355, 358 360, 380, 400 450, 500, 800
PP-COMM AP <sup>2</sup>	----	----	350, 360, 380 400, 500
PP-COMM AP <sup>3</sup> w/ TCP	----	----	400, 500, 950 1000
SC-UHP AP <sup>4</sup>	----	----	200, 400, 500 800, 1000
PP-UHP AP	PBAA	47 to 439	100, 300, 400 500, 600
PP-UHP AP	HTPB	37 to 94	300, 500
PP-UHP AP	PU	115	300, 500
PP-COMM AP	HTPB	100	300, 500
PP-COMM AP w/ TCP	HTPB	90 to 94	300, 500
SC-UHP AP	CTPB	55 and 192	300, 500

1. Pressed polycrystalline, ultra-high purity AP.
2. Pressed polycrystalline, commercial grade AP.
3. Pressed polycrystalline, commercial grade AP with TCP.
4. Single crystal, ultra-high purity AP.

TABLE III

## CONDITIONS FOR EXPERIMENTAL RUNS

Schlieren light source	1000 watt mercury vapor arc lamp
External lighting <sup>1</sup>	1200 watt SLM-1200 projector
Color film	Kodak Ektachrome 7241
Light-source chopper location	Just ahead of mercury vapor arc lamp
Knife edge	Blue and red filter matrix
Focusing lens	610 mm, f6
Framing rate	7500 PPS
Camera shutter	1/2.5

1. Film No. 31 had no external lighting.

TABLE IV

## EXPERIMENTAL RUN DATA

Film No.	AP Type	Binder Type	Binder Thickness (microns)	Pressure (psig)
27	UHP <sup>1</sup>	PBAA	81	300
28	UHP	PBAA	94	100
29	UHP	PBAA	86	400
30	UHP	PBAA	76	600
31	UHP	PBAA	94	300
32	UHP	PBAA	94	500
33	UHP	None	--	400
34	UHP	None	--	500
35	COMM <sup>2</sup>	None	--	400
36	COMM	None	--	500
37	SINGLE	None	--	400
38	SINGLE	None	--	500
39	UHP	PBAA	432	300
40	UHP	PBAA	439	500
41	UHP	PBAA	50	300
42	UHP	PBAA	47	500
43	UHP	HTPB	93	300
44	UHP	HTPB	94	500
45	COMM	HTPB	100	300
46	COMM	HTPB	99	500

TABLE IV (Continued)

Film No.	AP Type	Binder Type	Binder Thickness (microns)	Pressure (psig)
47	COMM w/ TCP	HTPB	90	300
48	COMM w/ TCP	HTPB	94	500
49	SINGLE	None	--	800
50	SINGLE	None	--	500
52	SINGLE	CTPB	192	300
53	SINGLE	CTPB	55	500
54	UHP	HTPB	64	300
55	UHP	HTPB	37	500
56	UHP	None	--	800
57	UHP	PU	114	300
58	UHP	PU	116	500
59	SINGLE	None	--	800
60	SINGLE	CTPB	27	500
61	SINGLE	None	--	1000
62	UHP	HTPB	112	500
63	SINGLE	None	--	500
64	SINGLE	None	--	200

1. UHP refers to pressed polycrystalline, ultra-high purity AP.
2. COMM refers to pressed polycrystalline commercial grade AP.
3. SINGLE refers to single crystal, ultra-high purity AP.

TABLE V

## SUMMARY OF DATA FROM FILMS

Propellant Grade	Binder Type	Binder Thickness	Pressure (psig)	Remarks
PP-UHP	---	---	400	(See Fig. 4) Peak temperature above center, spaces between reaction sites visible (approximately 300 microns in width.) Laminar deflagration and planar surface regression.
SC-UHP	---	---	400	(See Fig. 5) Peak temperature was above center and spaces between reaction sites visible (250 microns wide.) Subsurface phase change zone visible (approximately 200 microns in depth.)
PP-UHP	---	---	500	(See Fig. 7) Peak temperature above center, spaces between reaction sites visible. Gases less laminar than at 400 psig. Planar surface regression. Large scale mixing.
SC-UHP	---	---	500	(See Fig. 8) Spaces between reaction sites visible (approximately 400 microns in width.) Subsurface phase change zone visible, but unmeasurable.
PP-UHP	---	---	800	(See Fig. 10) More constant temperature across burner. Deflagration very turbulent. Spaces between reaction sites visible (460 microns.) Planar surface regression.
SC-UHP	---	---	800	(See Fig. 11) More turbulent than SC at 500 psig. Subsurface phase change zone more vague. Spaces between reaction sites visible (430 microns.) Planar surface regression.



TABLE V (Continued)

Propellant Grade	Binder Type	Binder Thickness	Pressure (psig)	Remarks
PP-COMM	---	---	400	(See Fig. 6) Peak temperature above burner. Much large scale mixing. Reaction sites were visible (450 microns.) Surface was irregular.
PP-COMM	---	---	500	(See Fig. 9) Deflagration appeared turbulent, with much large scale mixing. Spaces between reaction sites visible (450 microns.) Surface regression was planar.
PP-UHP	PBAA	Medium	100	(See Fig. 12) Deflagration was very laminar. Burned with a small, steady flame. Very little AP decomposition.
PP-UHP	PBAA	Thin	300	(See Fig. 13) Deflagration appeared laminar. Burned with a small, squat, bushy flame that fluctuated gently. Little or no mixing occurred for some distance above surface.
PP-UHP	PRAA	Medium	300	(See Fig. 14) Deflagration appeared laminar. Flame larger than thin binder at same pressure. Some temporal fluctuations of flame noted. Unsteadiness associated with spikes of AP.
PP-UHP	PBAA	Thick	300	(See Fig. 16) Flame was very large and very unsteady. Smoke and flame obscured much of the combustion process.
PP-UHP	PBAA	Medium	400	(See Fig. 17) Burned with an unsteady flame. Peak temperature above center of burner. Spaces between reaction sites visible. Flame taller than PP-UHP, medium binder thickness, at 300 psig.
PP-UHP	PBAA	Thin	500	(See Fig. 18) Deflagration appeared more laminar than turbulent. Flame was taller than thin binder at same pressure. Large scale mixing was prevalent.

TABLE V (Continued)

Propellant Grade	Binder Type	Binder Thickness	Pressure (psig)	Remarks
PP-UHP	PBAA	Medium	500	(See Fig. 19) Deflagration appeared turbulent. Flame fluctuated and was taller than thin binder at same pressure. More mixing than thin binder at same pressure.
PP-UHP	PBAA	Thick	500	(See Fig. 20) Burned with a large unsteady flame. Binder protruded well above the burner surface.
PP-UHP	PBAA	Medium	600	(See Fig. 21) Burned with a large unsteady flame. Gases above burner turbulent. Burner surface stepped and uneven. Spaces between reaction sites obscured.
PP-UHP	HTPB	Thin	300	(See Fig. 22) Burned with a small, bushy flame. Deflagration laminar. Surface was irregular. There was much mixing.
PP-UHP	HTPB	Medium	300	(See Fig. 23) Deflagration and pyrolysis appeared laminar. Taller flame than thin binder at same pressure. Surface regression was planar.
PP-COMM	HTPB	Medium	300	(See Fig. 24) Very irregular surface. AP pyrolysis was slow.
PP-UHP	HTPB	Thin	500	(See Fig. 25) Flame was unsteady. Surface regression was planar. Deflagration was turbulent.
PP-UHP	HTPB	Medium	500	(See Fig. 26) Flame was unsteady and appeared bushier than PBAA of same pressure and thickness. Less large scale mixing than thin binder at same pressure.
PP-COMM	HTPB	Medium	500	(See Fig. 27) Flame appeared much the same as UHP sandwiches at same pressure. Surface pyrolysis was very irregular.

TABLE V (Continued)

Propellant Grade	Binder Type	Binder Thickness	Pressure (psig)	Remarks
PP-UHP	PU	Medium	300	(See Fig. 28) Flame had same appearance as HTPB and PBAA thin binder at 300 psig. AP surface pyrolysis was laminar. Burned with a steady flame.
PP-UHP	PU	Medium	500	(See Fig. 29) Burned with an unsteady flame. Surface regression was planar. Binder protruded above surface. Turbulent deflagration.
SC-UHP	CTPB	Medium	300	(See Fig. 30) Burned with a large flame. Binder protruded well above the surface. Burned with an unsteady flame.
SC-UHP	CTPB	Thin	500	(See Fig. 31) Flame burned down rear of burner. Deflagration was turbulent. Very much large scale mixing was present.
SC-UHP	---	---	1000	(See Fig. 32) Extremely turbulent combustion. Reaction sites indistinct, estimated to be 150 microns in width. Subsurface zone was not visible.
PP-UHB	HTPB	Medium	500	(See Fig. 35) No color matrix used. Yellow color visible in gases above burner.
SC-UHP	---	---	500	(See Fig. 33) Horizontal color matrix used. Gas phase yellow-green color much reduced, not seen in many frames. Pulsating thermal layer type burning. Subsurface zone visible.
SC-UHP	---	---	200	(See Fig. 34) Wire-wrapped crystal. Yellow-green color visible where wire touches crystal on the blue (left) side.

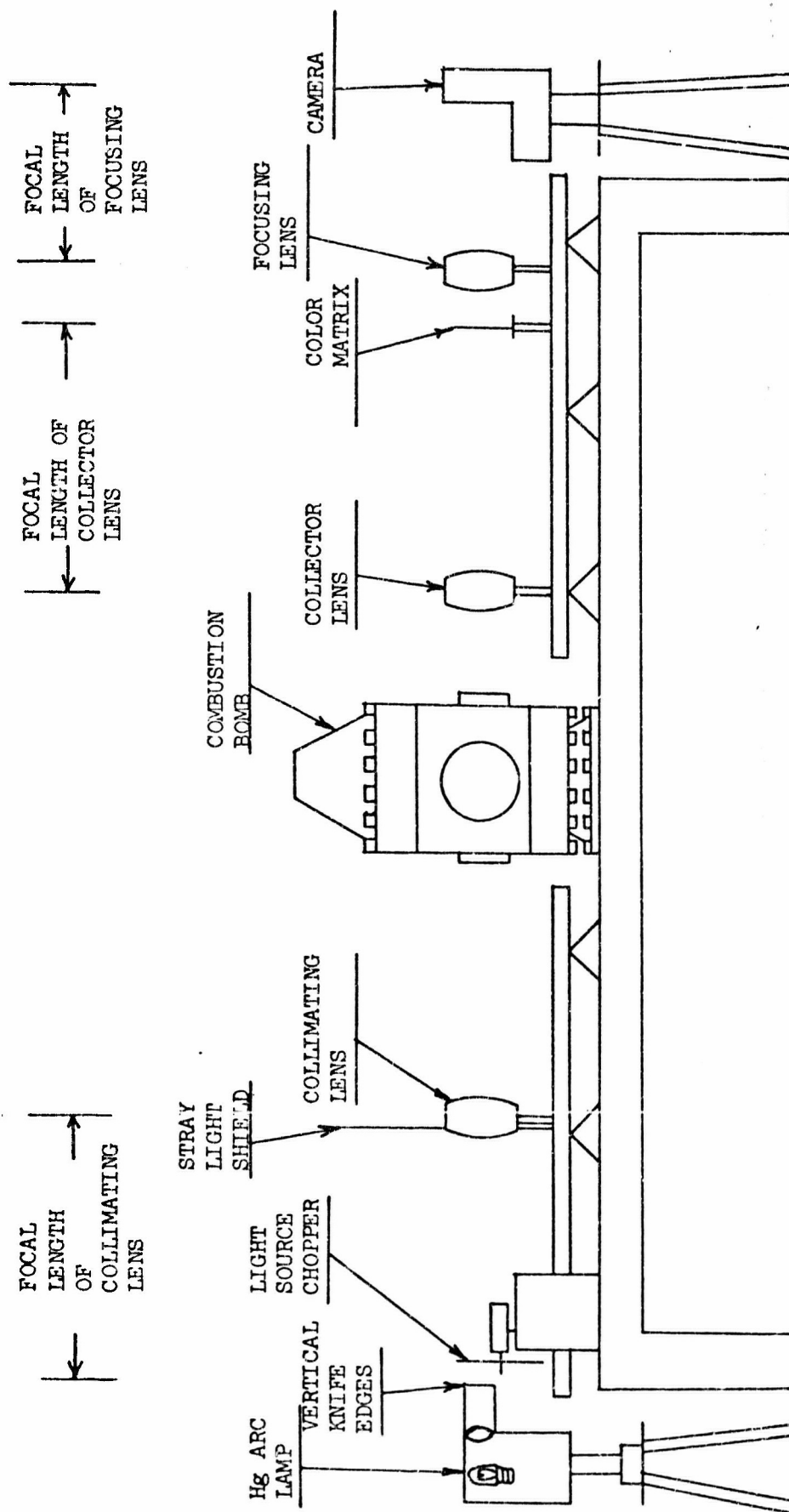


FIGURE 1. SCHEMATIC OF EQUIPMENT ARRANGEMENT

Reproduced from  
best available copy.

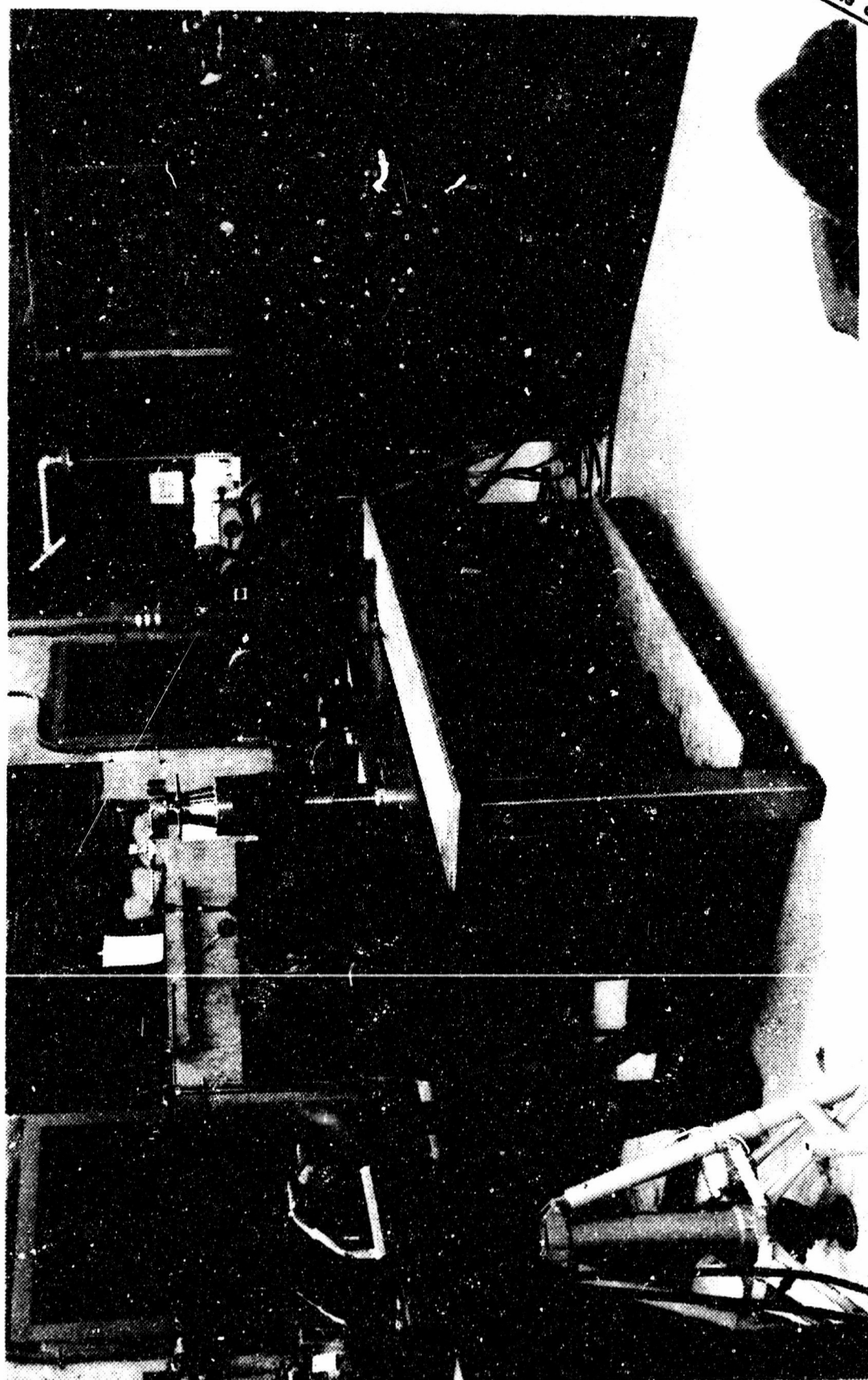


FIGURE 2. VIEW OF EQUIPMENT ARRANGEMENT

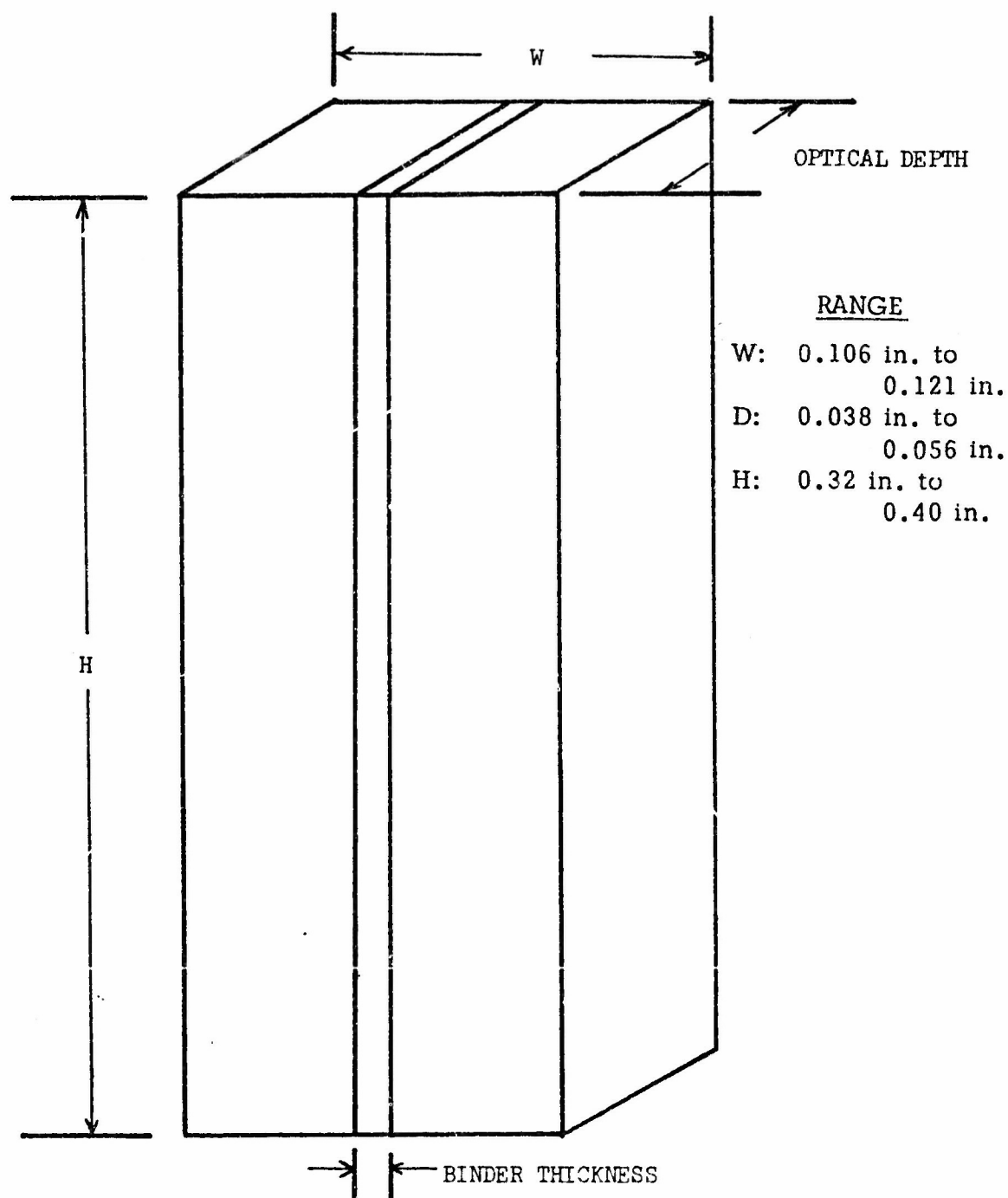


FIGURE 3. SANDWICH BURNER DIMENSIONS

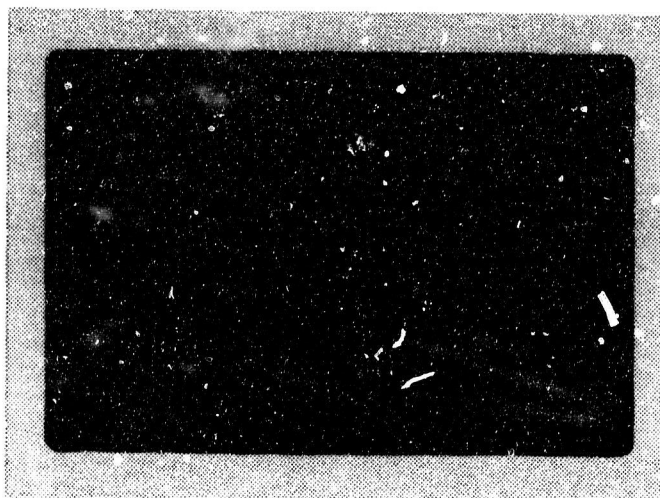


FIGURE 4. PP-UHP AP Burned at 400 psig

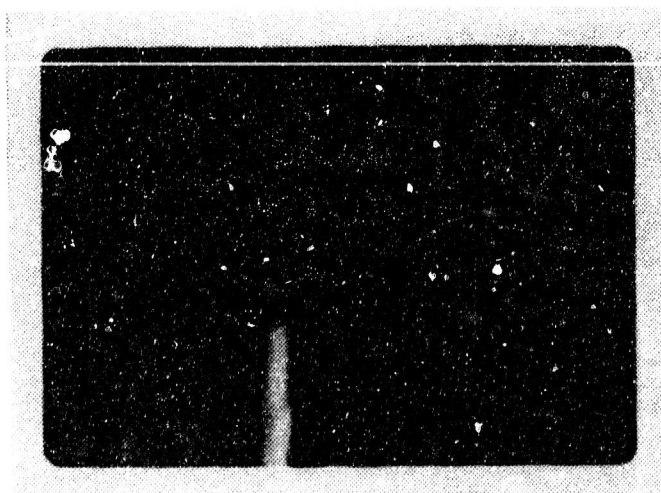


FIGURE 5. SC-UHP AP Burned at 400 psig



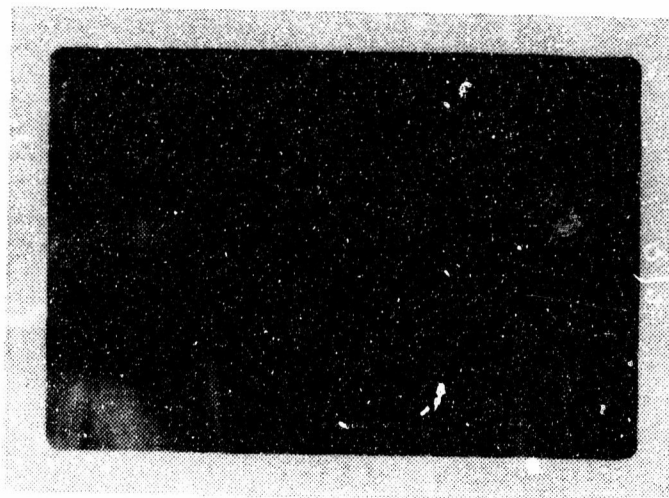


FIGURE 6. PP-COMM AP Burned at 400 psig

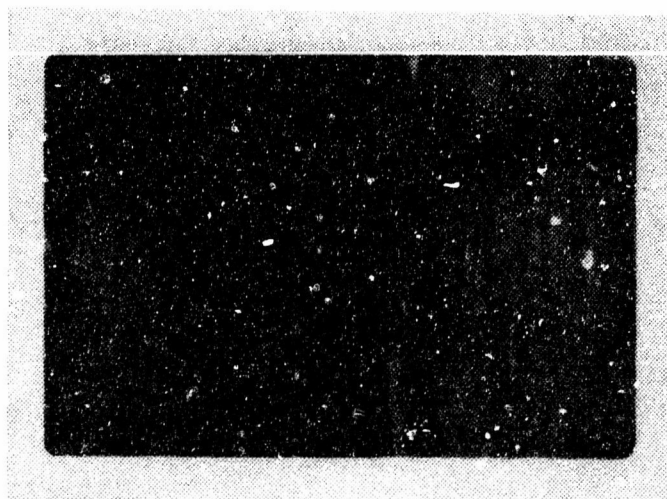


FIGURE 7. PP-UHP AP Burned at 500 psig



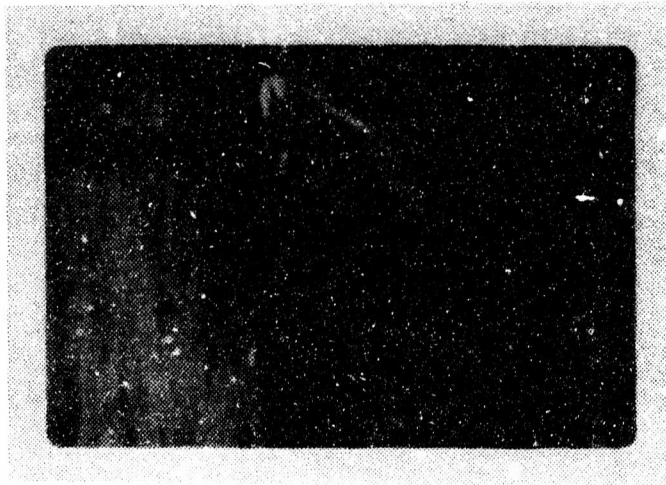


FIGURE 8. SC-UHP AP Burned at 500 psig

Reproduced from  
best available copy.

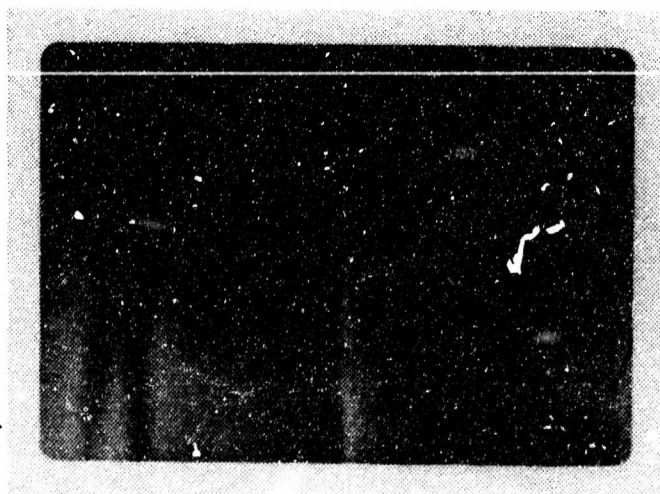


FIGURE 9. PP-COMM AP Burned at 500 psig

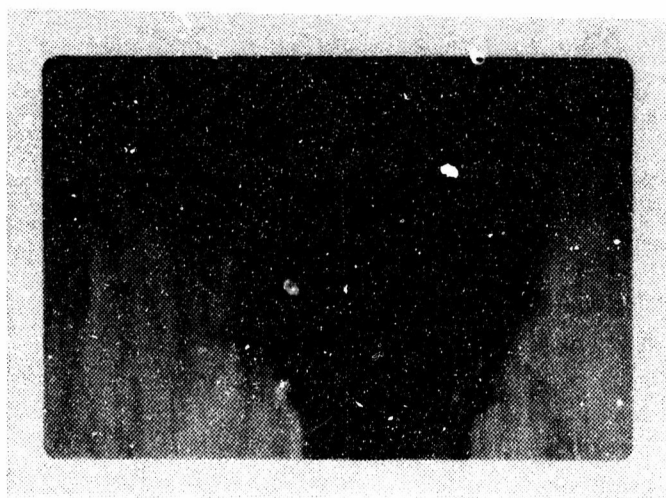


FIGURE 10. PP-UHP AP Burned at 600 psig



FIGURE 11. SC-UHP AP Burned at 800 psig



FIGURE 12. PP-UHP AP/PBAA, 94 micron binder, 100 psig

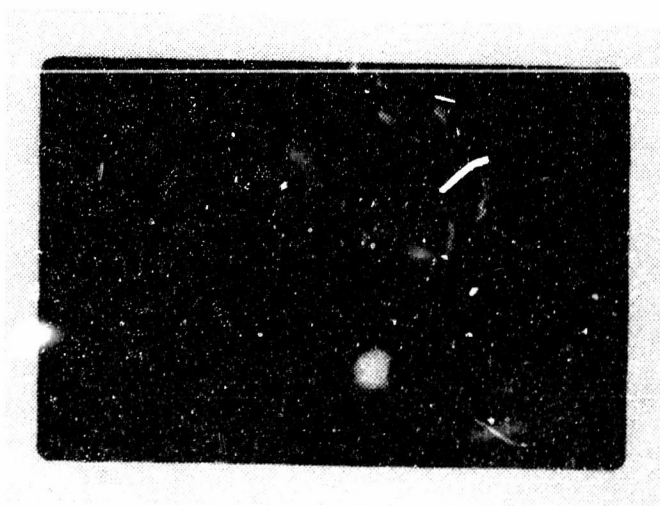


FIGURE 13. PP-UHP AP/PBAA, 50 micron binder, 300 psig



FIGURE 14. PP-UHP AP/PBAA, 81 micron binder, 300 psig

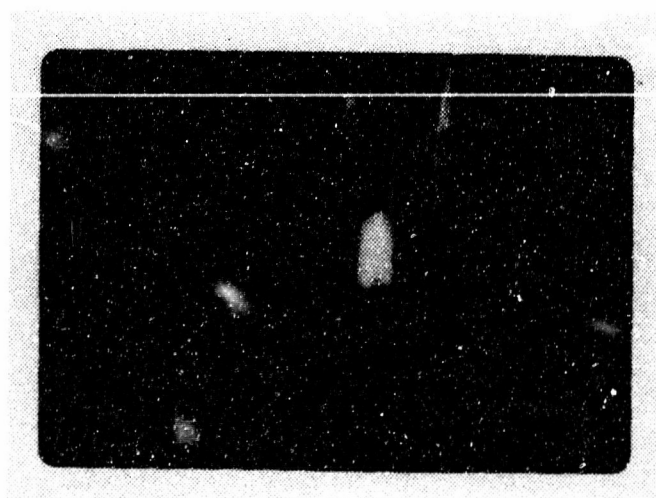


FIGURE 15. PP-UHP AP/PBAA, 94 micron binder, no side lighting,  
300 psig

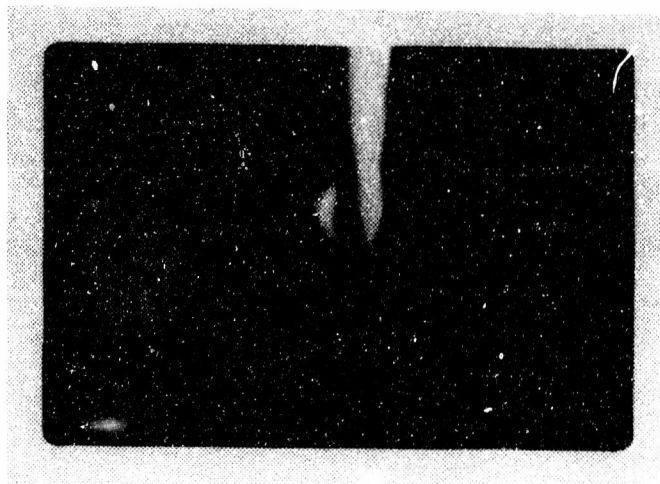


FIGURE 16. PP-UHP AP/PBAA, 432 micron binder, 300 psig

Reproduced from  
best available copy.



FIGURE 17. PP-UHP AP/PBAA, 86 micron binder, 400 psig

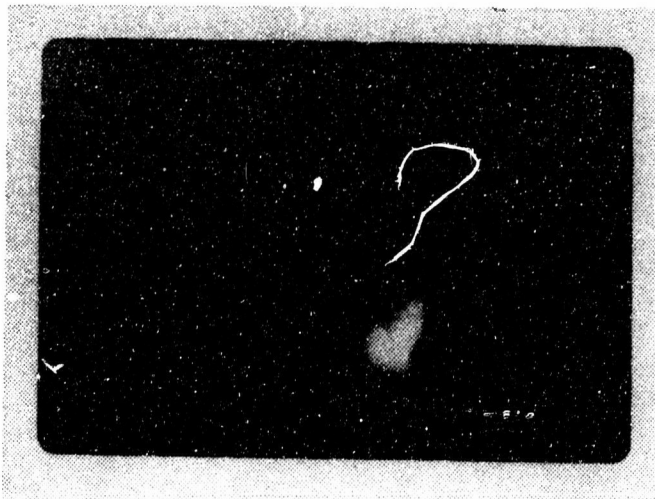


FIGURE 18. PP-UHP AP/PBAA, 47 micron binder, 500 psig

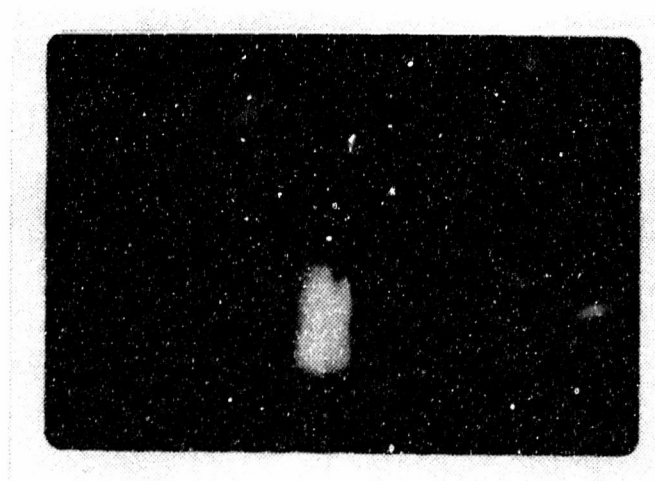


FIGURE 19. PP-UHP AP/PBAA, 94 micron binder, 500 psig

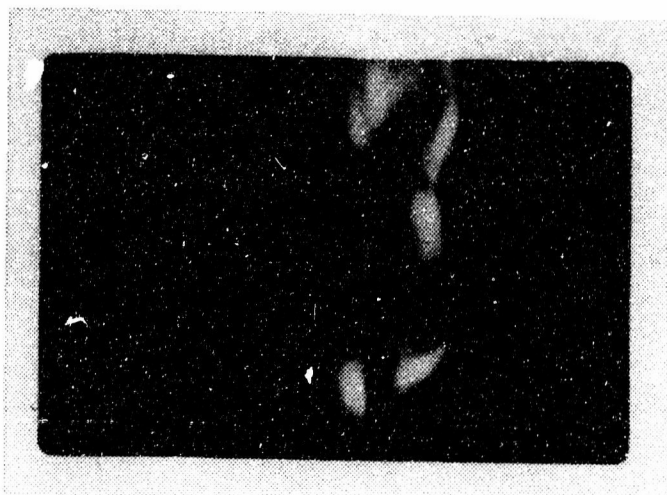


FIGURE 20. PP-UHP AP/PBAA, 439 micron binder, 500 psig

Reproduced from  
best available copy.

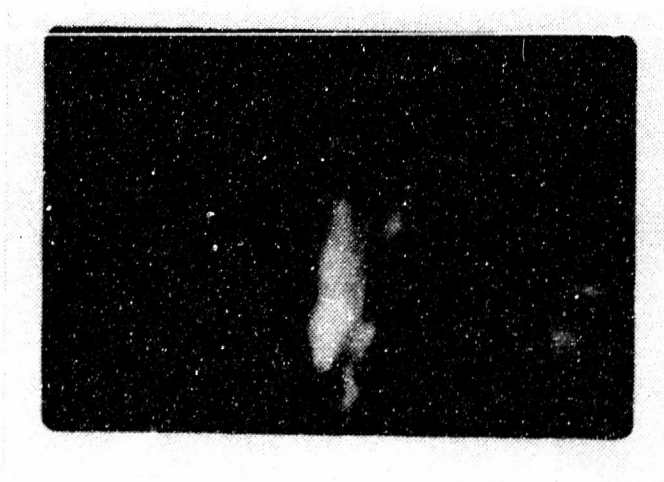


FIGURE 21. PP-UHP AP/PBAA, 76 micron binder, 600 psig



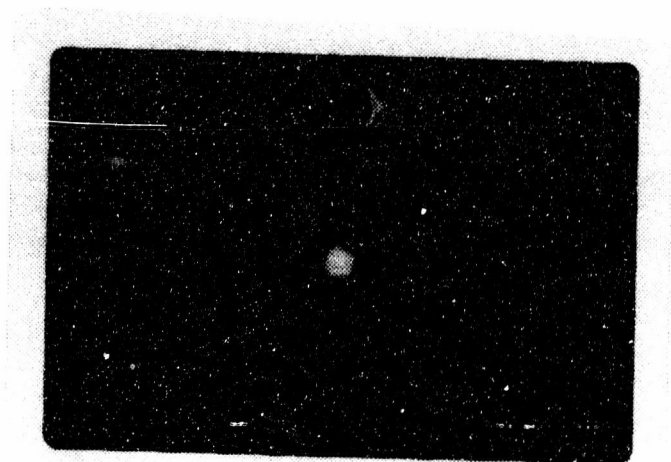


FIGURE 22. PP-UHP AP/HTPB, 64 micron binder, 300 psig



FIGURE 23. PP-UHB AP/HTPB, 93 micron binder, 300 psig





FIGURE 24. PP-COMM AP/HTPB, 100 micron binder, 300 psig

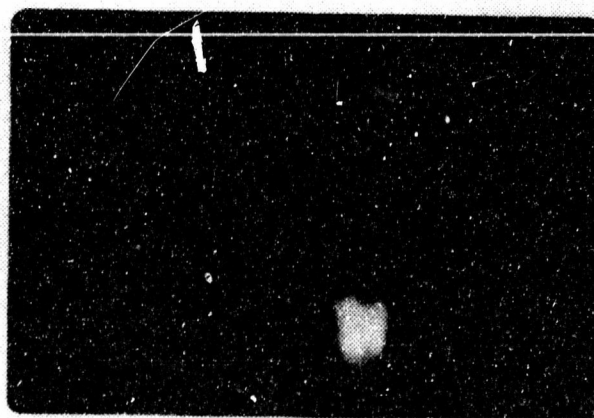


FIGURE 25. PP-UHP AP/HTPB, 37 micron binder, 500 psig

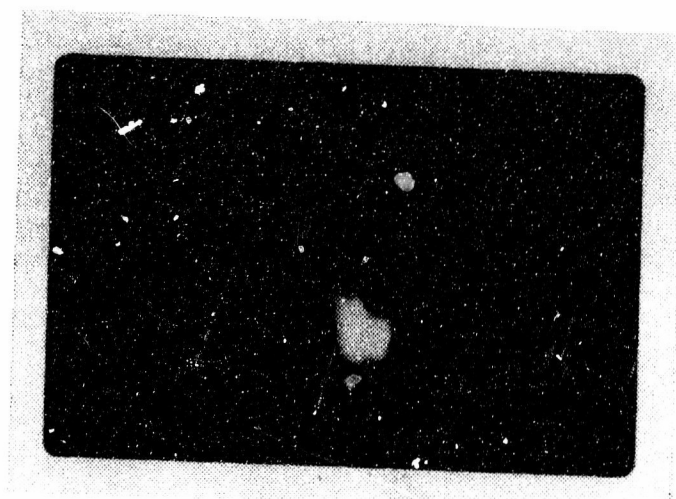


FIGURE 26. PP-UHP AP/HTPB, 94 micron binder, 500 psig

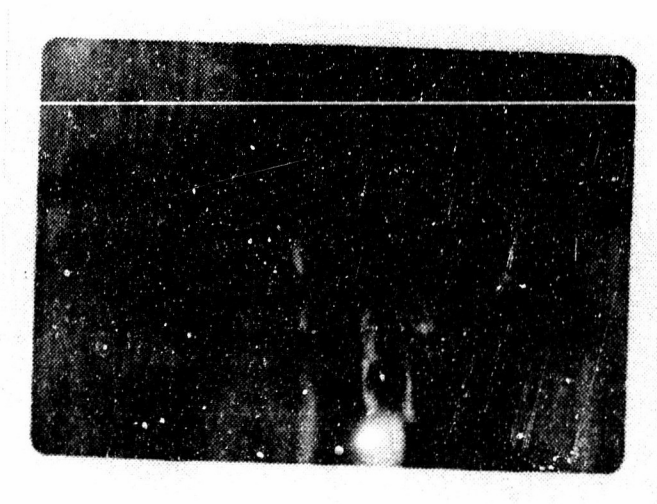


FIGURE 27. PP-COMM AP/HTPB, 99 micron binder, 500 psig

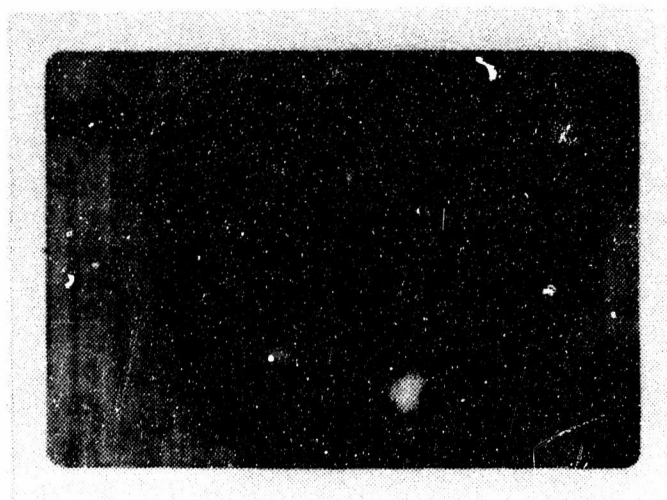


FIGURE 28. PP-UHP AP/PU, 114 micron binder, 300 psig

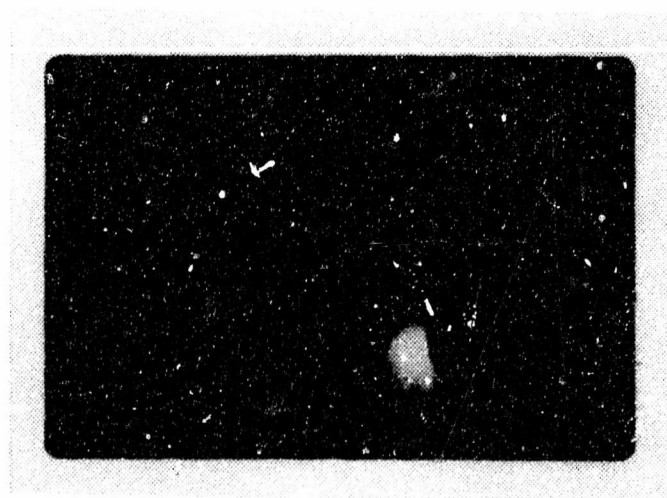


FIGURE 29. PP-UHP AP/PU, 116 micron binder, 500 psig

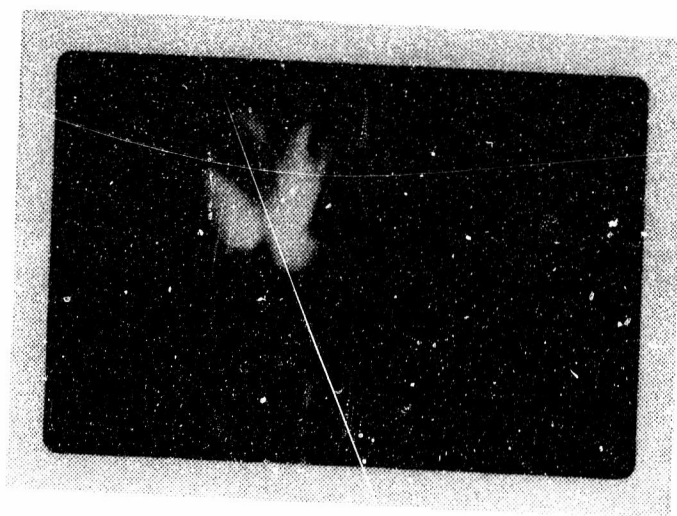


FIGURE 30. SC-UHP AP/CTPB, 192 micron binder, 300 psig

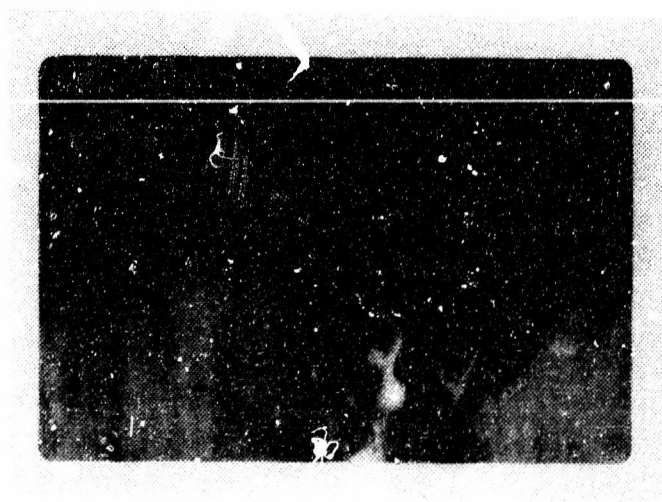


FIGURE 31. SC-UHP AP/CTPB, 55 micron binder, 500 psig

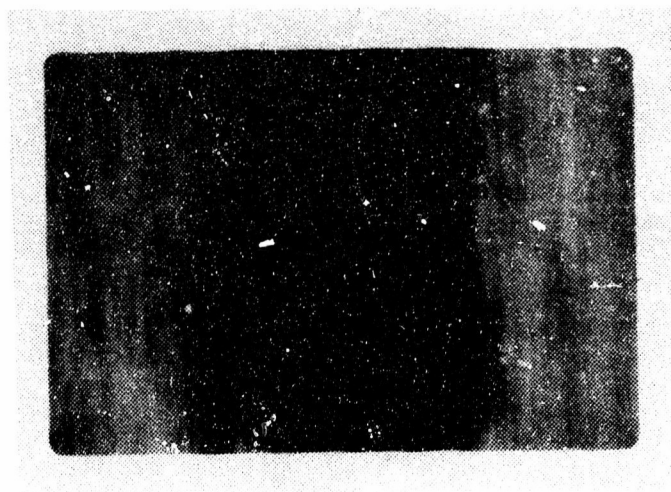


FIGURE 32. SC-UHP AP, Burned at 1000 psig

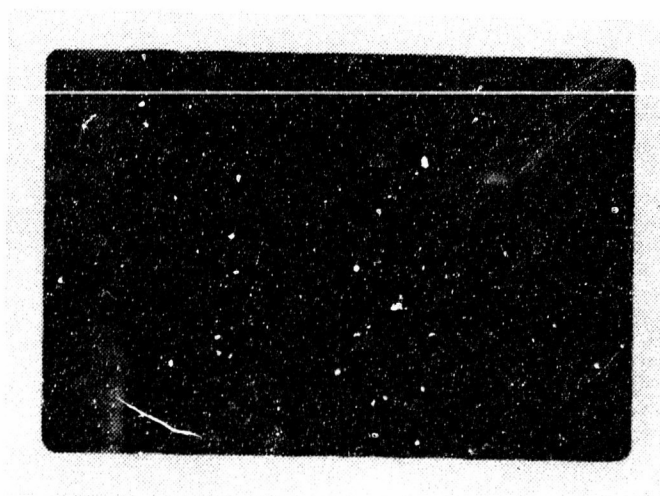


FIGURE 33. SC-UHP AP, Burned at 500 psig with a Horizontal Color Matrix



FIGURE 34. SC-UHP AP, 200 psig, Wire-wrapped Crystal

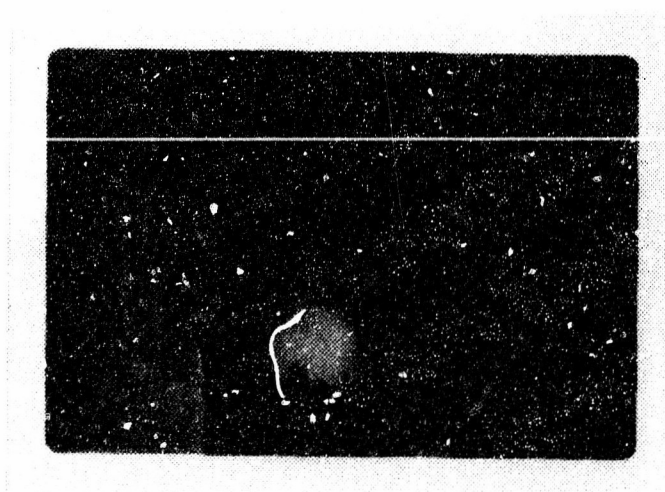


FIGURE 35. PP-UHP AP/HTPB, 60 micron binder, 500 psig,  
color matrix removed

## LIST OF REFERENCES

1. Varney, A. M., An Experimental Investigation of the Burning Mechanisms of Ammonium Perchlorate Composite Solid Propellants, Ph.D. Thesis, Georgia Institute of Technology, Atlanta, Georgia, 1970.
2. Hightower, J. D. and Price, E. W., "Experimental Studies Relating to the Combustion Mechanism of Composite Propellants," Astronautica Acta, v. 14, no. 1, p. 11-22, November 1968.
3. Derr, R. L. and Boggs, T. L., "Role of the Scanning Electron Microscope in the Study of Solid Propellant Combustion: Part III. The Surface Structure and Profile Characteristics of Burning Composite Solid Propellants," Combustion Science and Technology, v. 1, no. 5, p. 369-384, April 1970.
4. Boggs, T. L. and Kraeutle, K. J., "Role of the Scanning Electron Microscope in the Study of Solid Rocket Propellant Combustion, I: AP Decomposition and Deflagration," Combustion Science and Technology, v. 1, p. 75-93, 1969.
5. Boggs, T. L., "Deflagration Rate, Surface Structure, and Subsurface Profile of Self-Deflagrating Single Crystals of Ammonium Perchlorate," AIAA Journal, v. 8, no. 5, p. 867-873, May 1970.
6. Kennedy, J. R., An Optical Study of Ammonium Perchlorate Sandwiches with a Polybutadiene Acrylic Acid Binder, Ae.E. Thesis, Naval Postgraduate School, Monterey, California, 1972.
7. Boggs, T. L. and Zurn, D. E., "The Deflagration of Ammonium Perchlorate - Polymeric Binder Sandwich Models," Combustion Science and Technology, v. 4, p. 279-282, 1972.
8. Beckstead, M. W. and Hightower, J. D., "Surface Temperature of Deflagrating Ammonium Perchlorate Crystals," AIAA Journal, v. 5, no. 10, p. 1785-1790, 1967.



## BIBLIOGRAPHY

1. Gaydon, A. G. and Wolfhard, H. G., Flames - Their Structure, Radiation, and Temperature, 3d ed., Chapman and Hall, 1970.
2. Hesse, W. J. and Mumford, N. V. S. Jr., Jet Propulsion Aerospace Applications, 2nd ed., Pittman Publishing Corporation, 1964.
3. Ladenburg, R. W. (editor), Physical Measurements in Gas Dynamics and Combustion, Princeton University Press, 1954.
4. Netzer, D. W., Kennedy, J. R., Biery, G. M. II, and Brown, W. E., Nonmetalized Composite Propellant Combustion, Naval Post-Graduate School Report No. NPS 57NT72031A, March 1972.
5. Sutton, G. P., Rocket Propulsion Elements, 3d ed., John Wiley and Sons, 1958.
6. Weinberg, F. J., Optics of Flames, Butterworths, 1963.
7. Warren, F. A., Rocket Propellants, Reinhold Publishing Corporation, 1958.